Ring State for Single Transition Metal Atoms on Boron Nitride on Rh(111)

Fabian Donat Natterer, François Patthey, and Harald Brune

Institute of Condensed Matter Physics (ICMP), Ecole Polytechnique Fédérale de Lausanne (EPFL), CH-1015 Lausanne, Switzerland

(Received 11 April 2012; revised manuscript received 15 June 2012; published 7 August 2012; publisher error corrected 13 August 2012)

The low-temperature adsorption of isolated transition metal adatoms (Mn, Co, and Fe) onto hexagonal boron nitride monolayers on Rh(111) creates a bistable adsorption complex. The first state considerably weakens the hexagonal boron nitride- (*h*-BN-) substrate bond for 60 BN unit cells, leading to a highly symmetric ring in STM images, while the second state is imaged as a conventional adatom and leaves the BN-substrate interaction intact. We demonstrate reversible switching between the two states and, thus, controlled pinning and unpinning of the *h*-BN layer from the metal substrate. $I(z)$ and $d\ln I/dz$ curves are used to reveal the BN deformation in the ring state.

DOI: 10.1103/PhysRevLett.109.066101 PACS numbers: 68.35.Np, 62.23.Kn, 68.37.Ef

Monolayers of sp^2-hybridized honeycomb lattices, such as graphene and hexagonal boron nitride (*h*-BN), grown on close-packed single crystal surfaces are fascinating substrates, in particular in their role as novel hosts for adsorbed atoms, molecules, or nanostructures, but also due to their intrinsic electronic and structural properties. A prominent example is the moiré pattern formed by *h*-BN/Rh(111) $-$ (12×12) [1–6]. This system is characterized by highly inhomogeneous substrate binding of the different stacking areas of the moiré unit cell. The regions where N atoms are on top of Rh atoms are strongly bound due to the hybridization of the N lone pair orbital with the Rh *d*-states [6,7]. No such chemical bond is formed where N atoms are situated on the threefold Rh hollow sites. These stacking areas are, thus, only weakly bound by van der Waals interactions [7]. Since there is only one type of on-top site and two types of hollow sites, the ratio of both stacking areas is 1:2. This gives rise to strongly bound equidistant circular regions surrounded by a connected and weakly bound area, also called wires [1].

The transition between the differently bound parts of the layer occurs on a lateral scale of only two atomic rows [7]. Therefore, the structure essentially consists of two levels, disconnected hexagonal bound areas close to the Rh, surrounded by a connected honeycomb area lifted off the substrate by 1.0 Å [7]. This abrupt transition is untypical for moiré patterns, however, since the layer doesn't exhibit holes [3], we refer to it as a moiré pattern and not as a nanomesh. The inhomogeneous binding involves a splitting of the sp^2-derived σ and π bands by 1 eV [1,4,8] and nonuniform charge transfer from *h*-BN to Rh [7], leading to a spatial modulation of the work function [9–11] and to large lateral electric dipoles [10]. These dipoles exert electrostatic forces on polarizable adsorbates enabling the trapping of naphthalocyanine [4], of Cu-phthalocyanine [9], and of water [7,11] molecules, as well as of rare gas atoms [9,12]. Concerning metals, large Co clusters show preferred adsorption in the bound areas [13], but single metal atoms appear less well steered as they are predominately resting at the borders of the bound areas. Apart from a theoretical study for Au atoms revealing large binding energy differences [14], the interaction of metal atoms with the *h*-BN layer, as well as possible effects on the *h*-BN-substrate interaction, remain largely unexplored.

We report that single transition metal (TM) adatoms, namely Mn, Co, and Fe, adsorbed onto *h*-BN/Rh(111) $-$ (12×12), exhibit a bistable state at $T < 35$ K. The first state considerably weakens the *h*-BN substrate bond for 60 BN unit cells and is imaged in STM as a highly symmetric ring with 1.9 nm diameter that is centered in the moiré unit cell. Many rings have six symmetrically arranged protrusions, as shown in Fig. 1. The second state is imaged as a single and sharp protrusion (dot), as expected for a single adatom. We demonstrate reversible switching between the two states. Evidence for the adlayer substrate bond weakening is inferred from nonexponential current distance curves and from STM images.

The measurements were performed with a homemade STM, operating at 4.7 K and a base pressure below 5×10^{-11} mbar [15]. TM atoms were deposited from

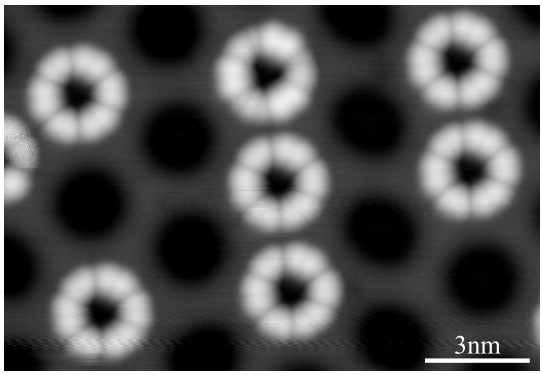

FIG. 1. STM image of highly symmetric rings centered at the apparent depressions of the *h*-BN/Rh(111) $-$ (12×12) moiré unit cell ($V_t = -0.10$ V and $I_t = 10$ pA).

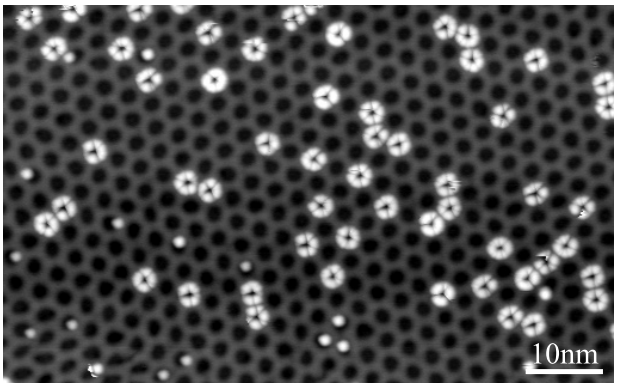

FIG. 2. STM image showing the coexistence of Mn rings with single protrusions (dots). [$\Theta = (1.71 \pm 0.03) \times 10^{-3}$ ML, $T_{\mathrm{dep}} = 10$ K, $V_t = -0.10$ V, and $I_t = 10$ pA].

high purity rods with an e-beam evaporator onto the sample in the STM position and at 10 K. The h-BN monolayer was prepared by exposing the clean Rh(111) surface [16] at 1040 K for 100 s to a borazine partial pressure of 2×10^{-7} mbar [1]. The resulting sample exhibits large and very well ordered h-BN regions coexisting with the clean metal substrate. The latter serves for a precise coverage calibration. On Rh(111), Co, and Fe are immobile at $T_{\mathrm{dep}} = 10$ K [17]. Hence, they exhibit statistical growth, leading for the low coverages used in the present study almost exclusively to single atoms; e.g., at the coverage of Fig. 2 the mean size is 1.005 [18]. Therefore, the density of adsorbates is equivalent to the coverage, given in monolayers, where one ML is defined as one adatom per Rh substrate atom. The indicated tunnel voltages V_t correspond to the sample potential. The $d\ln I/dz$ curves were measured by feeding the output of the IV-converter through a logarithmic amplifier into a Lock-In amplifier using a z-modulation of 16 pm peak-to-peak at 777 Hz.

Figure 1 shows highly symmetric rings observed after Mn deposition on h-BN/Rh(111) $-$ (12 × 12) at 10 K. Each ring exhibits six protrusions, every other of them with slightly different appearance giving rise to threefold symmetry. All rings are concentrically arranged around the apparent moiré depressions and have a diameter of (19.2 ± 0.2) Å, which is (0.59 ± 0.01) times the moiré period. Their apparent height with respect to the wires is 1.8 Å. Deposition of Fe and Co leads to rings with identical symmetry, diameter, and apparent height [19]. In what follows, we concentrate on Mn; however, the results are representative also for Co and Fe.

Figure 2 displays the coexistence of dot and ring state. In addition, there are asymmetric and incomplete rings. We attribute these different ring shapes to the varying TM atom position and to defects in the supporting h-BN. STM images of this kind are used to infer the average number of Mn atoms involved in both adsorption complexes. Deposition of a coverage Θ onto a surface with unit cells of size n leads to a probability $P_k = \binom{n}{k}\Theta^k(1-\Theta)^{n-k}$ of finding k atoms per unit cell [18]. For the present case of $n = 12 \times 12$ and the coverage of $\Theta = (1.71 \pm 0.03) \times 10^{-3}$ ML on the bare Rh(111) areas, we expect a fraction of $P_0 = (1-\Theta)^n = (0.782 \pm 0.004)$ empty moiré unit cells on the h-BN. However, we observe with (0.833 ± 0.004) a significantly higher amount. This can either be attributed to a sticking coefficient below unity on h-BN, or to an adatom mobility across moiré unit cells at the deposition temperature. Sticking coefficients below one have been reported for Co/h-BN/Ni(111) [20]. No sign of intercell adsorbate diffusion is observed when heating the sample beyond the deposition temperature. Therefore, we attribute the larger fraction of empty cells solely to the sticking coefficient. The experimentally observed quantity of empty moiré cells is obtained for a Mn coverage on h-BN of $\Theta = (1.27 \pm 0.03) \times 10^{-3}$ ML. The ratio of this coverage to the one on Rh yields an initial sticking coefficient of $s_0 = (0.74 \pm 0.03)$ for Mn on h-BN at 10 K and concomitantly a mean size of (1.09 ± 0.02) atoms per adsorption complex. Therefore, the majority of the rings and dots originate from a single TM adatom.

We show in Fig. 3 the reversible transformation of rings into dots proving that both are different appearances and states of the same TM adatom/h-BN complex [21]. The transformation of a dot into a ring is achieved by applying a positive voltage pulse (+ 1 V, feedback-loop open) with the tip positioned on top of the dot. The back transformation is induced by a current ramp from 10 pA to 220 pA at −0.1 V with the tip centered on the former dot position [22].

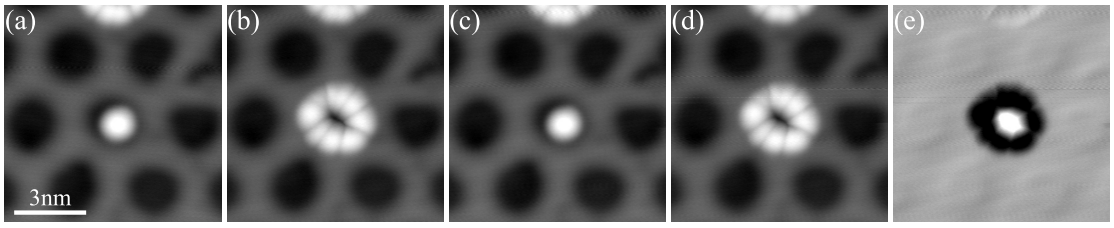

FIG. 3. Sequence of STM images, demonstrating the reversible transformation of a Mn dot into a ring and vice versa. (a)–(b) and (c)–(d) Switching a dot into a ring via a +1 V bias pulse applied at the center of the dot. (b)–(c) Transformation of a ring back into a dot via a current ramp at the former dot position ($V_t = -0.10$ V, ramp from 10 to 220 pA). Position and shape of dot and ring are unchanged. (e) Difference image of dot and ring indicates the adatom position. ($V_t = -0.10$ V and $I_t = 10$ pA).

A remarkable feature of these manipulations is that not only the dot and ring position, but also the internal ring structure are unchanged. Surprisingly, the adatom itself is hidden in STM images of the ring state. While we ignore the reason for the STM transparency of the TM atom in the ring state, we exclude the possibility that it is reversibly pushed below (ring) and pulled above the h-BN layer (dot), since once below, it is expected to bind much stronger to Rh.

Voltage pulses have been reported to modify the charge state and appearance of Au atoms on NaCl [23]. We, therefore, suggest the involvement of a charge difference between ring and dot state in the present study. However, the difference in appearance to the STM is much more striking in the present case. We note that 12 Xe atoms on h-BN/Rh(111) $-$ (12 $\times$ 12) have been shown to form rings with similar appearance [12] and, therefore, wish to stress that the present ring state is attributed to a single TM adatom only.

The following analysis shows how the TM adatom weakens the h-BN–substrate bonding in the ring state. The intriguing STM appearance is due to elastic deformation of the h-BN layer by tip-sample interactions and due to its intrinsic detachment from the substrate. Large deformations have been reported for tip-sample interactions acting on a soft membrane, such as freestanding [24] and SiO_2 supported [25] graphene. A signature of such deformations is that the true (s) and apparent (z) tip-sample distances are different, leading to deviations from exponential $I(z)$, respectively, constant $d\ln I/dz$ curves [26]. Figure 4 depicts

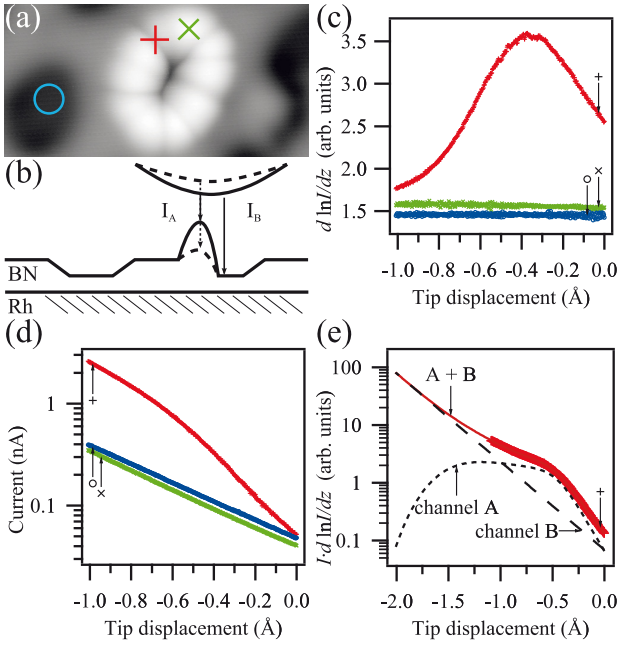

FIG. 4 (color online). (a) STM image of a Mn ring indicating the positions where (d) $I(z)$ and (c) $d\ln I/dz$ curves are recorded. (b) Parallel conduction channels A and B. (e) Product of curves (+) from (c) and (d) compared to a fit produced with Eqs. (1) and (2) ($V_t = -0.10$ V and $I_t = 20$ pA).

$I(z)$ and $d\ln I/dz$ curves recorded at three distinct positions. The current varies exponentially with tip displacement at the h-BN substrate (∘) and at the ring maxima (×). At the ring minima, however, $I(z)$ exhibits a change in slope and correspondingly $d\ln I/dz$ a large peak, see curves (+).

The exponential $I(z)$ curve over the h-BN is reminiscent of the tip-sample interaction being smaller than the h-BN-substrate interaction, whereas we attribute the exponential $I(z)$ signal above the ring maxima to the tip-sample interaction being stronger than the one between h-BN and substrate over the probed distance regime. Therefore, the h-BN monolayer is lifted off the substrate and attached to the tip, and the tunnel current is dominated by tunneling from this h-BN covered tip into Rh. Above the ring minima, the h-BN changes from being close to the sample at large z to being close to the tip at low z. Therefore, this regime allows us to assess the relative strength of both interactions. The current can be modeled by a superposition of two conduction channels. Channel A describes tunneling into the flexible membrane and, therefore, $s \neq z$, and channel B is tunneling across the h-BN into the underlying metal substrate. This yields

$$-\frac{I}{2}\frac{d\ln I}{dz} = \kappa_A I_A \left(\frac{dz}{ds}\right)^{-1} + \kappa_B I_B, \qquad (1)$$

where $\kappa_{A,B}$ are decay lengths of the respective wave functions [26]. dz and ds can be related by describing the tip-sample interaction with a Morse potential [26]:

$$\frac{dz}{ds} = 1 - \beta[\exp(-\kappa\Delta s) - 2\exp(-2\kappa\Delta s)], \qquad (2)$$

where Δs is the gap width relative to the point where the force between tip and sample is zero. The stability of the tunnel junction is governed by the parameter β that expresses the tip-sample stiffness [26,27]. A plot of $Id\ln I/dz$ is shown in Fig. 4(e). The experimental values of curve (+) are well described by the model as indicated by the full curve. The model permits to disentangle the contributions of both conduction channels and to extract $\beta = 7.5 \pm 1.0$. This value is close to the upper limit for stability [27] and about ten times larger than in Ref. [26], where tip and sample consisted of tungsten and silicon, respectively. This scales reasonably with the Young's moduli of the respective materials of $E_{BN} = 27$ GPa [28], $E_W = 340$ GPa, and $E_{Si} = 120$ GPa [26].

The most prominent features of the ring state are the maxima. As outlined above, their appearance is caused by tip-sample interactions and an intrinsic weakening of the h-BN substrate bond. We now show evidence for the latter. Figure 5 compares two STM images, one recorded at a common gap resistance of $R_g = 10^9$ Ω, and one very far from the surface at $R_g = 2 \times 10^{11}$ Ω. From the line profile it is seen that one of the maxima deflects by almost 1.5 Å upon changing the tip-sample separation, whereas the apparent height of the other maximum is unaffected. This strongly suggests that the latter maximum represents an intrinsic deformation of the h-BN layer. Notice that the ring is located

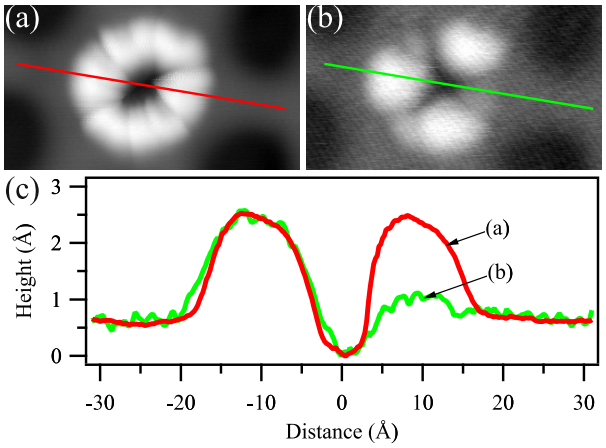

FIG. 5 (color online). STM images of the same Mn ring at (a) small and (b) large tip sample separation. While on one maximum, the *h*-BN membrane deflects by 1.5 Å between the two images, the other appears unchanged. (c) Line profiles. [$V_t = -0.10$ V, (a) $I_t = 100$ pA, and (b) $I_t = 0.5$ pA].

at the transition from the strongly to the weakly bound *h*-BN, and surprisingly, it is this transition region that gets detached in the ring state, while the weakly bound wires remain unaffected. This can be seen from the apparent heights of the wire areas between adjacent rings equaling the ones around empty moiré cells in Fig. 1. We note that a local weakening of the *h*-BN/Rh bond has been calculated for Au adsorption [14]; however, the present weakening goes far beyond in magnitude and in spatial extent.

In summary, the low-temperature deposition of small amounts of transition metal atoms (Mn, Fe, and Co) leads to a distribution of single adatoms on *h*-BN/Rh(111). Such a doping drastically influences the bonding of the *h*-BN layer to the metal substrate. A single TM adatom weakens the interaction of more than 60 surrounding *h*-BN unit cells to the underlying metal. The adsorption complex can be switched between the dot and the ring state and thereby the *h*-BN layer can be pinned to and un-pinned from the metal substrate in a reversible and controlled fashion.

We gratefully acknowledge funding from the Swiss National Science Foundation and discussions with M. Iannuzzi, P. Blaha, and F. Mittendorfer.

[1] M. Corso, W. Auwärter, M. Muntwiler, A. Tamai, T. Greber, and J. Osterwalder, Science **303**, 217 (2004).
[2] O. Bunk, M. Corso, D. Martoccia, R. Herger, P. R. Willmott, B. D. Patterson, J. Osterwalder, J. F. v. d. Veen, and T. Greber, Surf. Sci. **601**, L7 (2007).
[3] R. Laskowski, P. Blaha, T. Gallauner, and K. H. Schwarz, Phys. Rev. Lett. **98**, 106802 (2007).
[4] S. Berner, M. Corso, R. Widmer, O. Gröning, R. Laskowski, P. Blaha, K. Schwarz, A. Goriachko, H. Over, S. Gsell, M. Schreck, H. Sachdev, T. Greber, and J. Osterwalder, Angew. Chem., Int. Ed. **46**, 5115 (2007).
[5] R. Laskowski and P. Blaha, J. Phys. Condens. Matter **20**, 064207 (2008).
[6] A. B. Preobrajenski, A. S. Vinogradov, May Ling Ng, E. Ćavar, R. Westerström, A. Mikkelsen, E. Lundgren, and N. Mårtensson, Phys. Rev. B **75**, 245412 (2007).
[7] Y. Ding, M. Iannuzzi, and J. Hutter, J. Phys. Chem. C **115**, 13685 (2011).
[8] T. Brugger, H. Ma, M. Iannuzzi, S. Berner, A. Winkler, J. Hutter, J. Osterwalder, and T. Greber, Angew. Chem., Int. Ed. **49**, 6120 (2010).
[9] H. Dil, J. Lobo-Checa, R. Laskowski, P. Blaha, S. Berner, J. Osterwalder, and T. Greber, Science **319**, 1824 (2008).
[10] T. Greber, M. Corso, and J. Osterwalder, Surf. Sci. **603**, 1373 (2009).
[11] H. Ma, T. Brugger, S. Berner, Y. Ding, M. Iannuzzi, J. Hutter, J. Osterwalder, and T. Greber, Chem. Phys. Chem. **11**, 399 (2010).
[12] R. Widmer, D. Passerone, T. Mattle, H. Sachdev, and O. Gröning, Nanoscale **2**, 502 (2010).
[13] J. Zhang, V. Sessi, C. H. Michaelis, I. Brihuega, J. Honolka, K. Kern, R. Skomski, X. Chen, G. Rojas, and A. Enders, Phys. Rev. B **78**, 165430 (2008).
[14] H. P. Koch, R. Laskowski, P. Blaha, and K. Schwarz, Phys. Rev. B **84**, 245410 (2011).
[15] R. Gaisch, J. K. Gimzewski, B. Reihl, R. R. Schlittler, M. Tschudy, and W. D. Schneider, Ultramicroscopy **42–44**, 1621 (1992).
[16] The Rh(111) single-crystal was cleaned by cycles of Ar^+ ion sputtering (300 K, 30 min, 10 μA/cm^2, 1 kV), annealing in oxygen (815 K, 5 min, 2×10^{-7} mbar), and flashed to 1450 K.
[17] P. Blonski, A. Lehnert, S. Dennler, S. Rusponi, M. Etzkorn, G. Moulas, P. Bencok, P. Gambardella, H. Brune, and J. Hafner, Phys. Rev. B **81**, 104426 (2010).
[18] H. Brune, Surf. Sci. Rep. **31**, 121 (1998).
[19] Ti, Cr, Cu, and Au do not show such a ring state.
[20] W. Auwärter, M. Muntwiler, T. Greber, and J. Osterwalder, Surf. Sci. **511**, 379 (2002).
[21] Further evidence for rings and dots being different appearances of the same entity comes from their respective densities. While the ring and dot densities strongly vary from one STM image to another, their sum is constant within the error bar.
[22] All three adsorbates can be removed by a voltage pulse, which is element specific and independent of polarity in the ring state: $|V_{\mathrm{Mn}}| = 1.7 \pm 0.1$ V, $|V_{\mathrm{Fe}}| \approx 0.6$ V, $|V_{\mathrm{Co}}| = 0.4 \pm 0.2$ V.
[23] J. Repp, G. Meyer, F. E. Olsson, and M. Persson, Science **305**, 493 (2004).
[24] C. Lee, X. Wei, J. W. Kysar, and J. Hone, Science **321**, 385 (2008).
[25] T. Mashoff, M. Pratzer, V. Geringer, T. J. Echtermeyer, M. C. Lemme, M. Liebmann, and M. Morgenstern, Nano Lett. **10**, 461 (2010).
[26] C. J. Chen and R. J. Hamers, J. Vac. Sci. Technol. B **9**, 503 (1991).
[27] C. J. Chen, *Introduction to Scanning Tunneling Microscopy* (Oxford University Press, New York, 1993).
[28] A. Bosak, J. Serrano, M. Krisch, K. Watanabe, T. Taniguchi, and H. Kanda, Phys. Rev. B **73**, 041402 (2006).